

UNCLASSIFIED

AD. 4 6 1 8 3 9

DEFENSE DOCUMENTATION CENTER

FOR

SCIENTIFIC AND TECHNICAL INFORMATION

CAMERON STATION ALEXANDRIA, VIRGINIA



UNCLASSIFIED

NOTICE: When government or other drawings, specifications or other data are used for any purpose other than in connection with a definitely related government procurement operation, the U. S. Government thereby incurs no responsibility, nor any obligation whatsoever; and the fact that the Government may have formulated, furnished, or in any way supplied the said drawings, specifications, or other data is not to be regarded by implication or otherwise as in any manner licensing the holder or any other person or corporation, or conveying any rights or permission to manufacture, use or sell any patented invention that may in any way be related thereto.

461839

CATALOGED BY: DDC  
AS AN

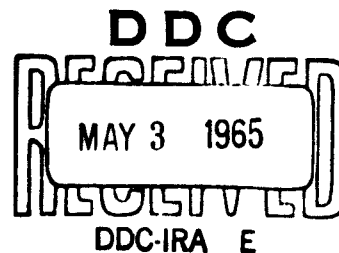
461839

U. S. NAVAL ORDNANCE LABORATORY  
White Oak, Silver Spring, Maryland

QUARTERLY PROGRESS REPORT ON ABRES RESEARCH

NOL BALLISTICS RANGE PROGRAM

20 January 1965 - 20 April 1965



U. S. NAVAL ORDNANCE LABORATORY  
White Oak, Silver Spring, Maryland

QUARTERLY PROGRESS REPORT ON ABRES RESEARCH  
NOL BALLISTICS RANGE PROGRAM

I. INTRODUCTION

The purpose of this program is to characterize the aerodynamic properties of the boundary layers and wakes of slender hypersonic vehicles by means of ballistics range data and their attendant analysis.

The Ballistics Range Program reported in this document is a portion of the ABRES program that is being provided by the U. S. Naval Ordnance Laboratory, White Oak, Maryland.

The NOL investigations have the following general objectives.

1. Measurement of aerodynamic properties that characterize the boundary layers and wakes of slender vehicles.
2. Evaluation of the experimental data to compare with existing theories.
3. Modification of current theory as required in the interpretation of the experiments.

II. PROGRAM

A. Task Identification

The major tasks, as identified in the Statement of Work, are as follows:

Task 1.0 Program Management

Task 2.0 Measurement of Turbulent Skin Friction on a Slender Cone

Task 3.0 Effect of High Heat Transfer Rates on Boundary Layer Transition

Task 4.0 Body-Scale Effects on the Aerodynamic Characteristics of Wakes

Task 5.0 The Effect of Heat Transfer on the Aerodynamic Characteristics of Wakes

The subjects under Task 1.0 are discussed in parts I, II, and III of this document.

Technical progress, problem areas and methods of solution for major tasks 2.0 through 5.0 are each discussed in part IV under their respective task numbers.

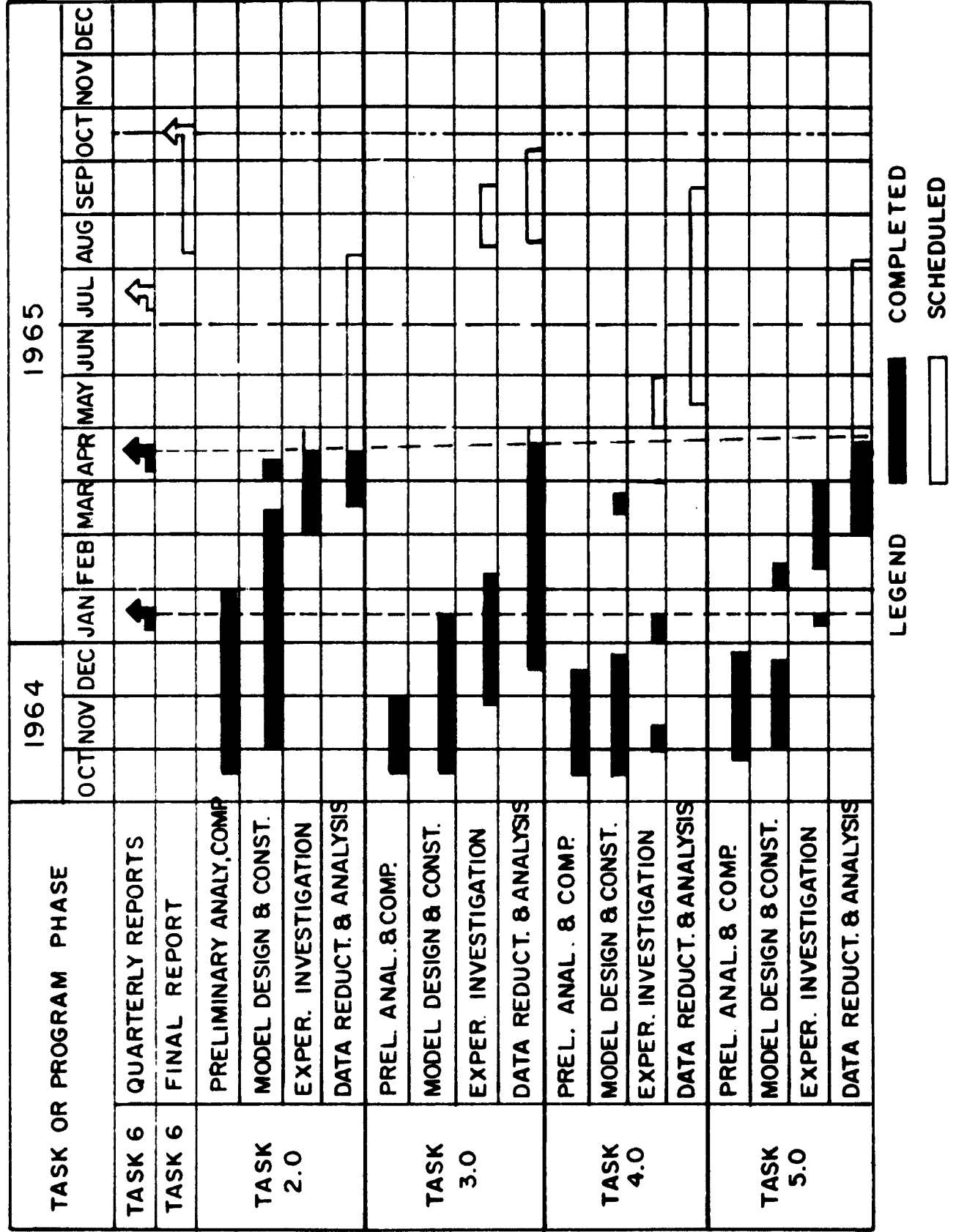
#### B. Schedules

The proposed schedules for major tasks and subtasks are presented in Table 1.1. The current plan of approach and the degree of completion of subtasks are outlined in this table.

### III. EXPERIMENTAL FACILITIES

All experimental tasks in the NOL Ballistics Range Program will be carried out in either the NOL Hyperballistics Range No. 4 or in the NOL Pressurized Ballistics Range No. 3. The general characteristics of these facilities are presented in the first quarterly report on this program. Specific capabilities of importance to individual tasks are discussed under appropriate task headings in part IV of this report.

# TABLE I.I



#### IV. STATUS OF NOL BALLISTICS RANGE PROGRAMS

##### A. Task 2.0 Measurement of Turbulent Skin Friction on a Slender Cone

The experimental phase of this program consists of launching slender conical models at hypersonic velocities into the NOL 1,000-foot Hyperballistics Range No. 4. The Reynolds number for these tests is sufficiently high to produce natural boundary layer transition very near the nose of the model so that almost the entire body is covered with a turbulent boundary layer. A total drag coefficient is determined for each successful launching. Theoretical values for the pressure drag coefficient component, the base drag coefficient component, and the skin friction drag coefficient component due to some laminar flow over the model are computed for each test. The difference between the sum of these computed drag coefficient components and the measured total drag coefficient is considered as the turbulent skin friction drag coefficient.

The models for these tests are 6.3-degree half-angle cones with a nose to base radius ratio of 0.03. Two different size models have been designed and fabricated: a homogeneous steel model with a base diameter of 1.25 inches and a copper nosed, titanium skirt model with a 1.00-inch base diameter. Figure 2.1 is a photograph of models of these two configurations with their sabots.

Part of the experimental portion of this program has been completed. Although the original test plan called for launchings at Mach numbers of 7, 10, and 15, the actual test Mach numbers have deviated slightly. Tests have been completed at Mach numbers between 6.71 and 9.59. The Mach number and other data for each test are listed in Table 2.1. The Reynolds numbers for these tests have varied between  $20.7 \times 10^6$  for the Mach number 6.71 test to  $29.6 \times 10^6$  for a Mach number 9.53 test. Values for the total drag coefficients have been obtained for each test. A preliminary analysis of these data has been in progress. The following is a description of this analysis.

The measured total drag coefficients which have been obtained from this program have been compared with theoretically calculated total drag coefficients. The theoretical total drag coefficients have been obtained by summing computed drag coefficient components for the pressure drag, the base drag, the skin friction drag due to a laminar boundary layer over a portion of the body, and the skin friction drag due to a turbulent boundary layer over the remainder of the body. The pressure drag coefficient was computed simply by integrating a value for the inviscid cone pressure over the surface of the cone and nondimensionalizing by the base area and the dynamic pressure. The base drag coefficient was obtained by assuming

that the base pressure was constant over the base and equal to one-tenth the free-stream pressure. The skin friction drag was obtained by integrating the proper component of the local shear stress over the body and then properly nondimensionalizing the results. The laminar shear stresses or skin friction coefficients were obtained as described in reference (2.1). The turbulent shear stresses were obtained by a similar method developed by Dr. R. E. Wilson of NOL. Although the maximum mean squared angle of attack for any of the launchings being reported was only one degree squared (less than one-half degree squared for many launchings), a correction was made to the measured drag coefficients to reduce them to zero angle of attack values. It was assumed that the drag coefficient varied linearly with the mean squared angle of attack and that the slope of this linear variation was invariant with either Mach number or Reynolds number. This assumption has been validated by the results presented in references (2.1) and (2.2). The slope used for this data reduction was 0.0012 per degree squared.

In order to compute the skin friction drag coefficients it was necessary to specify a value for the transition Reynolds number. Transition Reynolds numbers for the configuration being used in these tests were reported in reference (2.2) for Mach numbers of 9 and 13.3. Utilizing these data, a linear extrapolation was used to obtain transition Reynolds numbers at the required lower Mach numbers. The boundary layer could be seen on the models in the shadowgraph photographs taken during each launching. Boundary-layer transition was occurring so near the nose, however, that the exact location of transition was obscured by the bow shock wave lying very close to the surface. Fortunately when transition occurs very near the nose, variations in the transition Reynolds number do not appreciably affect the total drag of a slender cone. This is shown in figure 2.3 where calculated total drag coefficient has been plotted against the transition Reynolds number for three nominal Mach numbers and Reynolds numbers about which the data are grouped. The symbol in the center of each curve represents the transition Reynolds number for which each of the three curves in figure 2.2 were calculated. The symbols at each end of the curves represent transition Reynolds numbers that would have resulted in transition occurring one-half inch forward and one-half inch aft of the assumed location corresponding to the midpoint. The maximum variation in the total drag coefficient due to a transition fluctuation of one inch on the model is 0.9 percent. It therefore appears that it is not critical to know the exact location of transition.

To better establish the relation between the transition Reynolds number and the Mach number, a launching has been made at a Mach number of 8.5 and another one is planned for a Mach number of 6.5. The test conducted at a Mach number of 8.5 utilized a range pressure of 250 mm Hg. This resulted in boundary-layer transition occurring on the aft half of the model where the location can be easily determined from the



shadowgraph pictures made during the test. These data are currently being reduced but are not yet available for this report.

It was also deemed necessary to evaluate the effect of slight variations in the nose bluntness on the total drag coefficient. The models used in these tests were manufactured with a nose to base radius ratio of 0.03. Although the nose of the models was obscured in the shadowgraph pictures by the bow shock wave and some apparent luminosity, an attempt was made to measure the nose bluntness for the models at the end of their measured flight. For the highest Mach number case, preliminary measurements resulted in a maximum apparent bluntness ratio of 0.07. It is considered that for reasons mentioned previously, this is larger than the actual bluntness of the models. Using this as an upper limit, however, and referring to figure 2.4, it can be seen that a variation in bluntness ratio between 0.03 and 0.07 results in a maximum variation in the drag coefficient of only 1.25 percent. It is considered that this variation in bluntness is larger than was actually experienced during these tests.

Figures 2.5 through 2.9 represent typical data photographs used to obtain the results just discussed.

Figure 2.5 is a typical spark shadowgraph taken at a Mach number of 6.71. The very definite indications of turbulent boundary layer can be seen over most of the model surface.

Although the exact location of transition is difficult to observe because of the small shock angles resulting in narrow flow regions near the nose, it is apparent that transition is occurring near the nose.

The same conditions are evident at other range stations and other Mach numbers. This is illustrated by figures 2.6 and 2.7 for Mach 8.08 and by figure 7.8 for Mach number 9.53.

The shadowgraph of figure 2.8 must be examined carefully to establish that transition is taking place close to the model nose. Figure 2.9, however, a schlieren photograph of the same test, indicates clearly the turbulent nature of the boundary layer over all of the model except for a small area close to the nose.

Development effort is presently under way to improve loading conditions in the light gas launchers to obtain optimum velocities and launch acceleration rates for the high Mach number phase of the program.

## References

- 2.1 Lyons, Jr., W. C., Brady, J. J., and Levensteins, Z. J., "Hypersonic Drag, Stability, and Wake Data for Cones and Spheres," AIAA Journal, Vol. 2, No. 11, November 1964.
- 2.2 Sheetz, Jr., N. W., "Free-Flight Boundary-Layer Transition Investigations at Hypersonic Speeds," AIAA Paper No. 65-127, presented Second Aerospace Sciences Meeting, January 1965.

TABLE 2.1 REPRESENTATIVE SHOTS AT LOW AND INTERMEDIATE MACH NUMBERS

Shot No.	Mach No.	Range Pressure	Measured Drag Coefficient	$R_{0.1} \times 10^{-6}$	$\overline{\delta^2}$
698	7.94	1 atmosphere	.0706	24.0	.3
700	8.08	1 atmosphere	.0693	25.0	.5
701	7.81	1 atmosphere	.0706	24.0	.4
702	9.47	1 atmosphere	.0616	29.0	1.
710	9.53	1 atmosphere	.0615	29.5	0.4
711	6.71	1 atmosphere	.0791	20.7	1.
715	9.59	1 atmosphere	.0602	23.8	1.

$R_{0.1}$  = Reynolds number based upon free stream condition  
and model length

$$\overline{\delta^2} = [\text{Mean average angle of attack}]^2$$

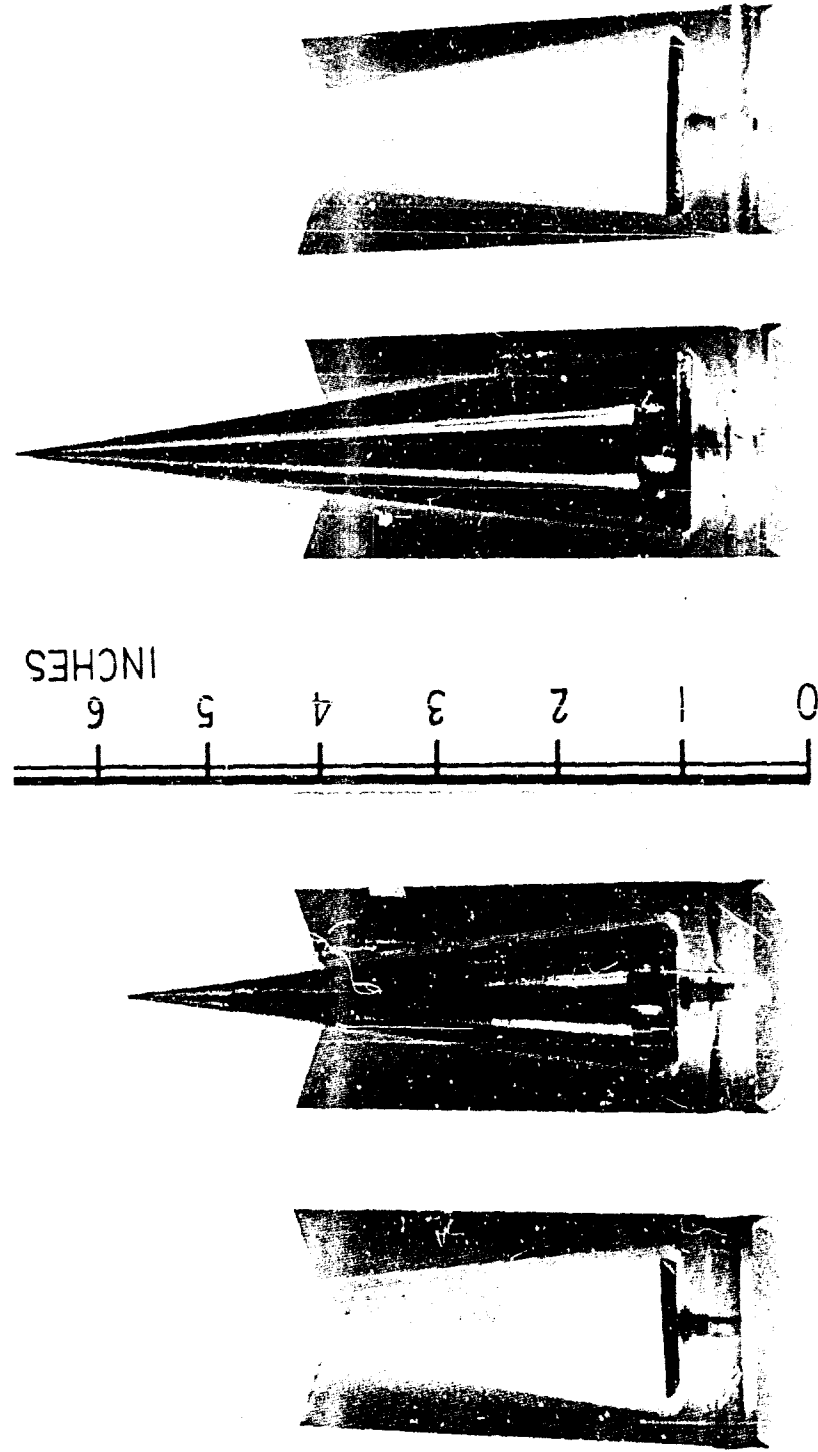


FIG. 2.1 MODEL AND SABOT CONFIGURATIONS FOR  
INTERMEDIATE (LEFT) AND LOW (RIGHT)  
MACH NUMBER PHASES OF TASK 2.

$\theta_c = 6.3$  DEGREES  
 $R_N/R_B = 0.03$

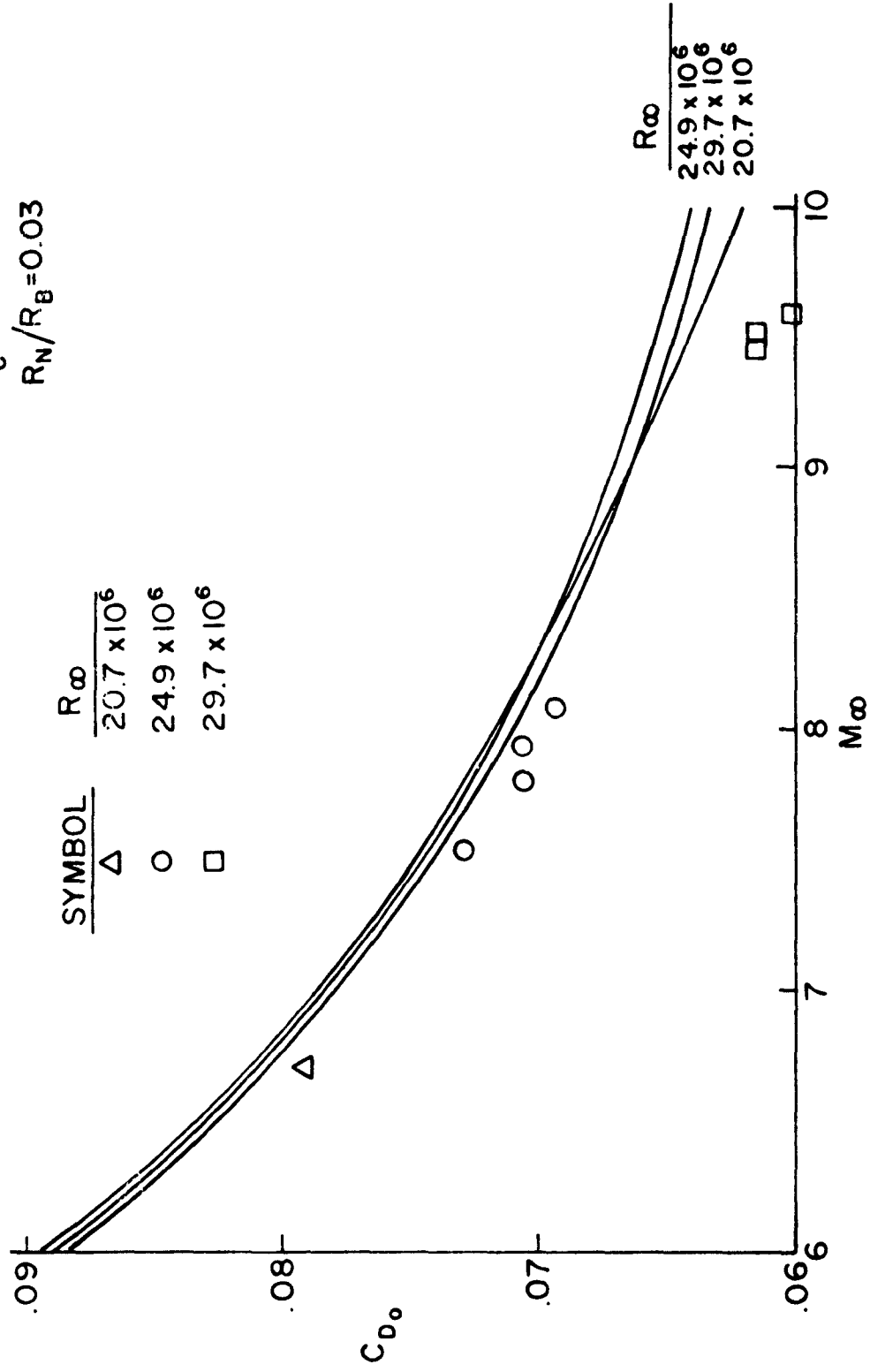


FIG. 2.2 COMPARISON OF EXPERIMENTAL TOTAL DRAG COEFFICIENTS WITH THEORY FOR A SLIGHTLY BLUNTED SLENDER CONE.

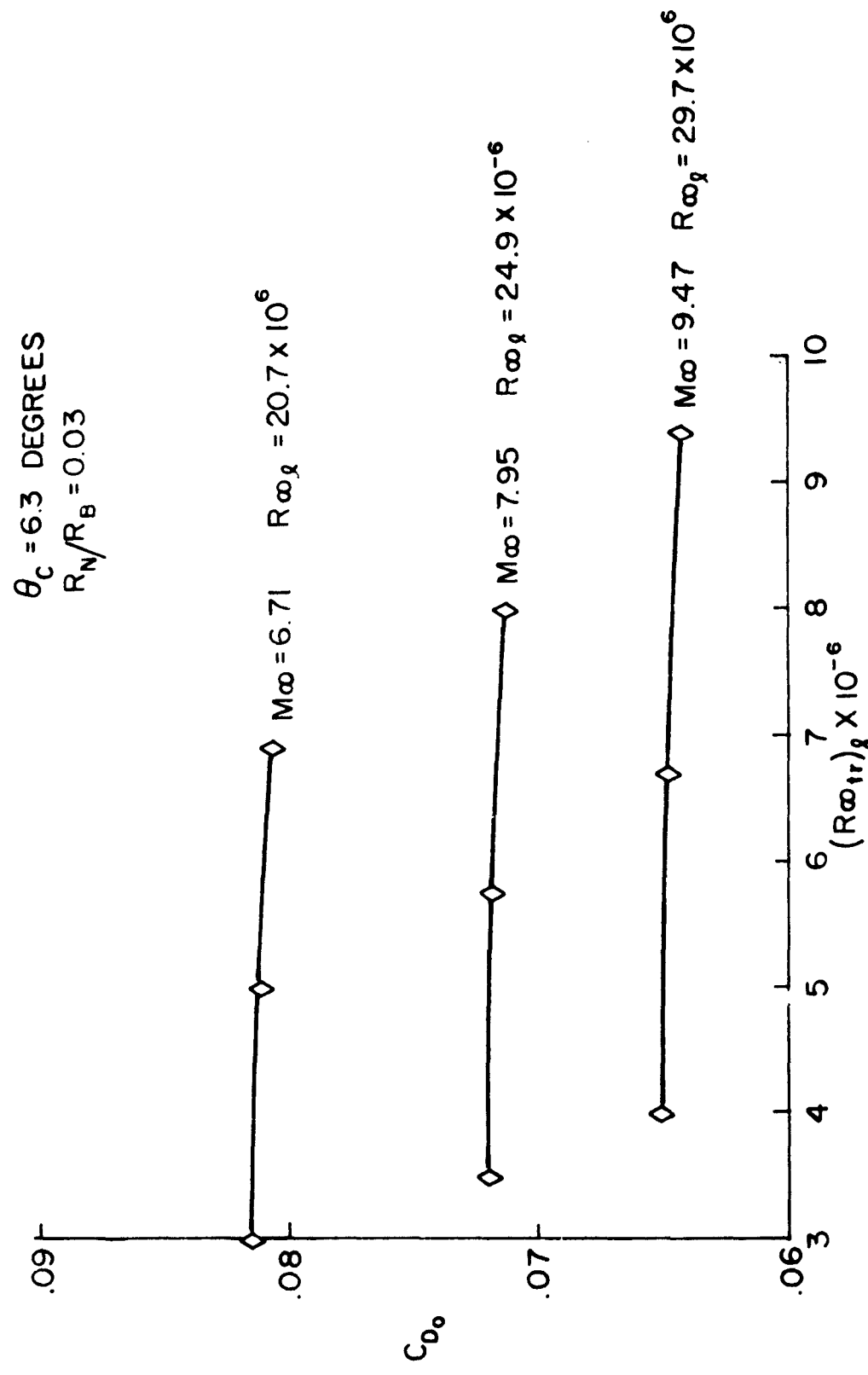


FIG. 2.3 EFFECT OF TRANSITION REYNOLDS NUMBER ON THE  
 TOTAL DRAG COEFFICIENT FOR A SLIGHTLY BLUNTED  
 SLENDER CONE.

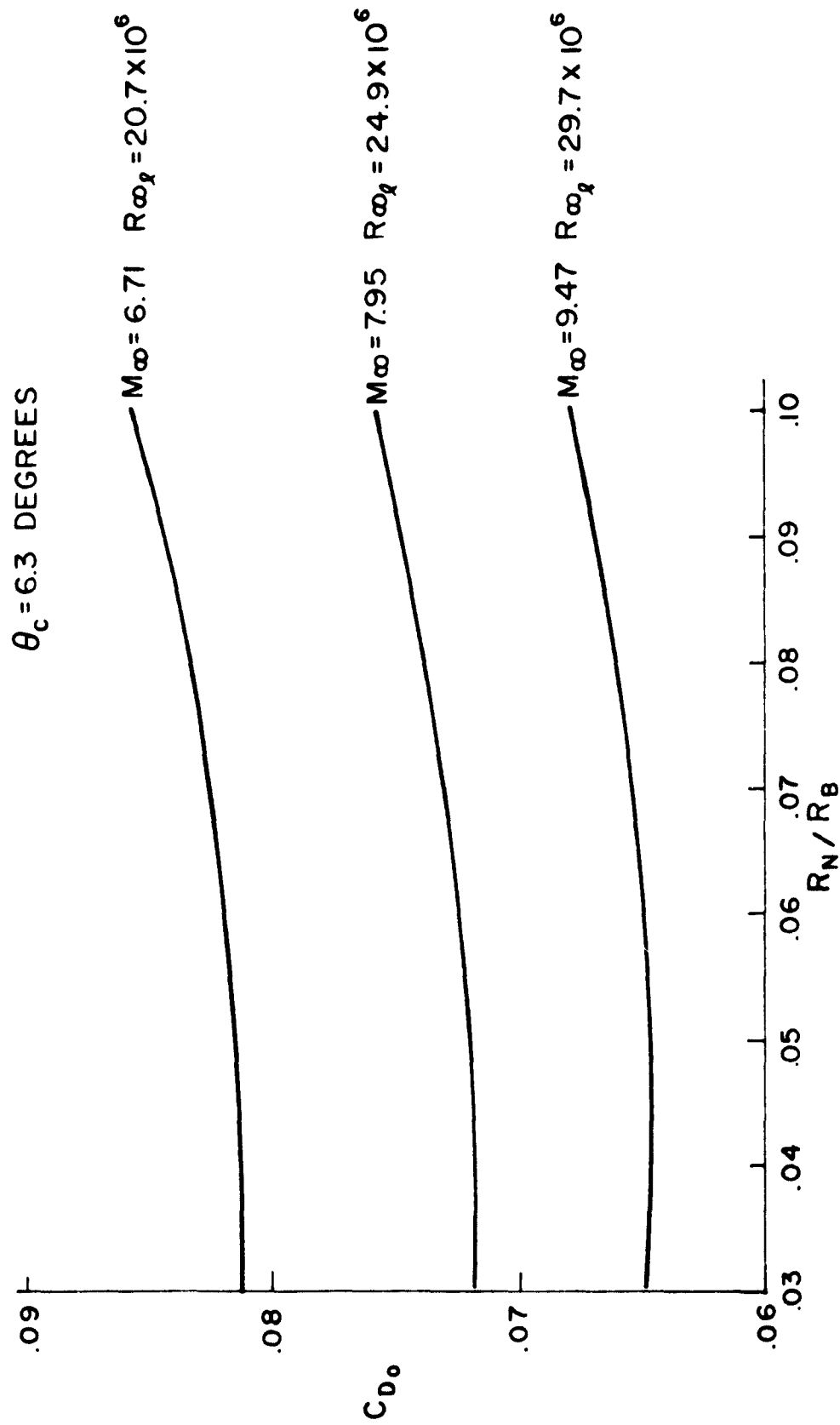


FIG. 2.4 EFFECT OF NOSE BLUNTNESS ON THE TOTAL DRAG COEFFICIENT FOR A SLIGHTLY BLUNTED SLENDER CONE.

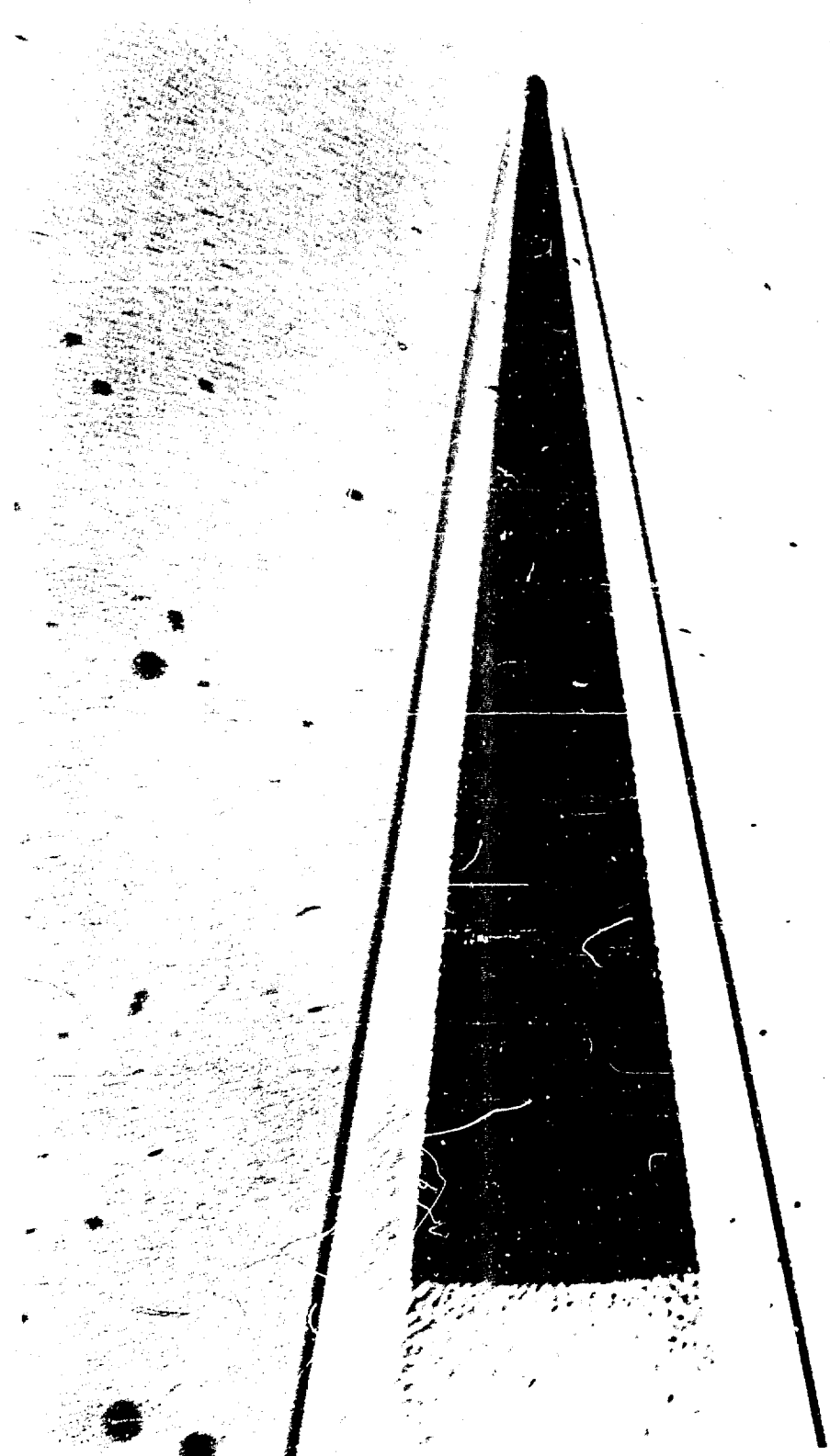


FIG. 2.5 SHADOWGRAPH OF MODEL FLYING AT  
STATION 340. MACH NUMBER 6.71  
SHOT • No. 711.



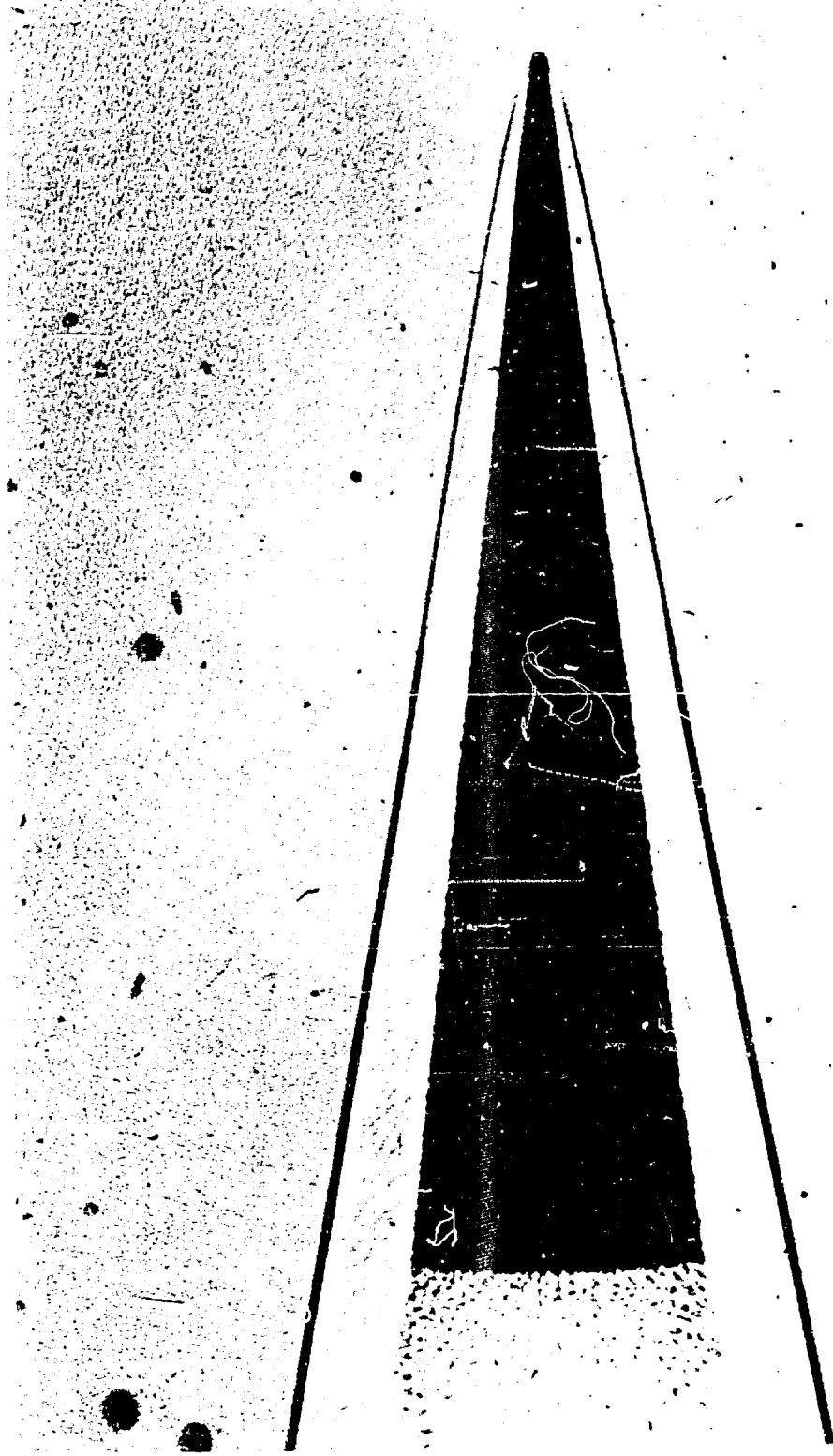


FIG. 2.5 SHADOWGRAPH OF MODEL FLYING AT  
STATION 340. MACH NUMBER 6.71  
SHOT • No. 711. •

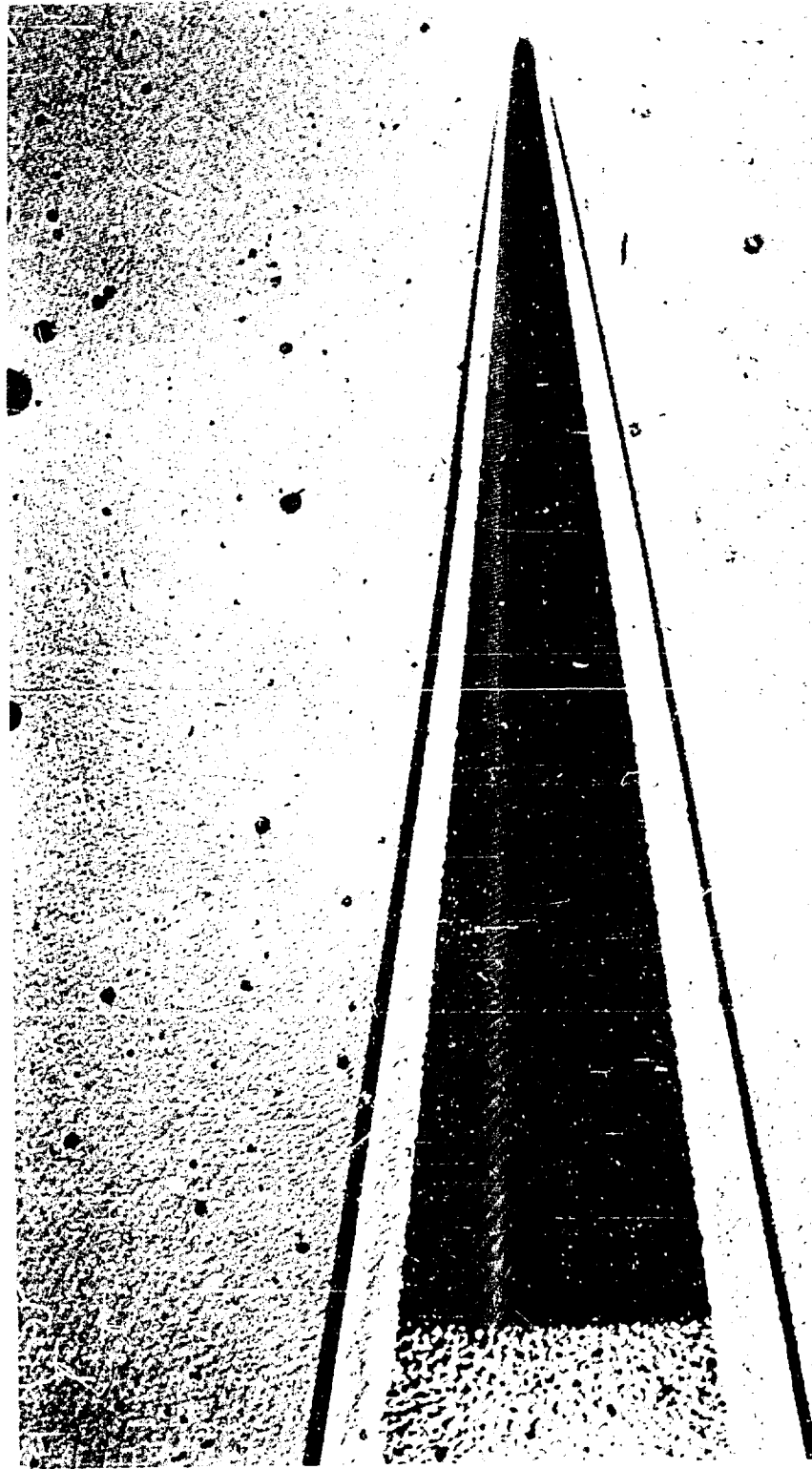


FIG. 2.6 SHADOWGRAPH OF MODEL FLYING AT  
STATION 080. MACH NUMBER 8.08  
SHOT No. 700.

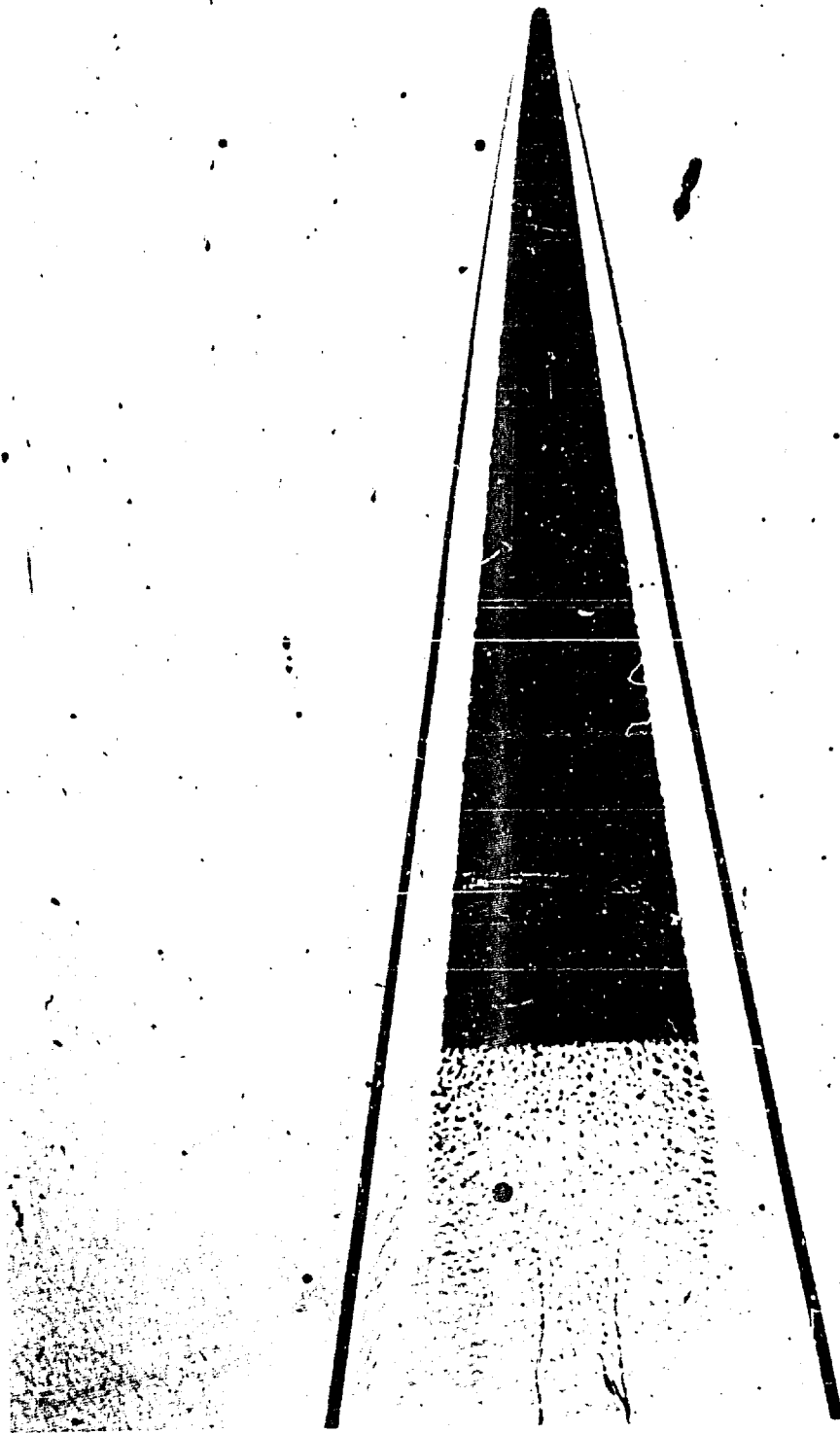


FIG. 2.7 SHADOWGRAPH OF MODEL FLYING AT  
STATION 387. MACH NUMBER 8.08  
SHOT No. 700.

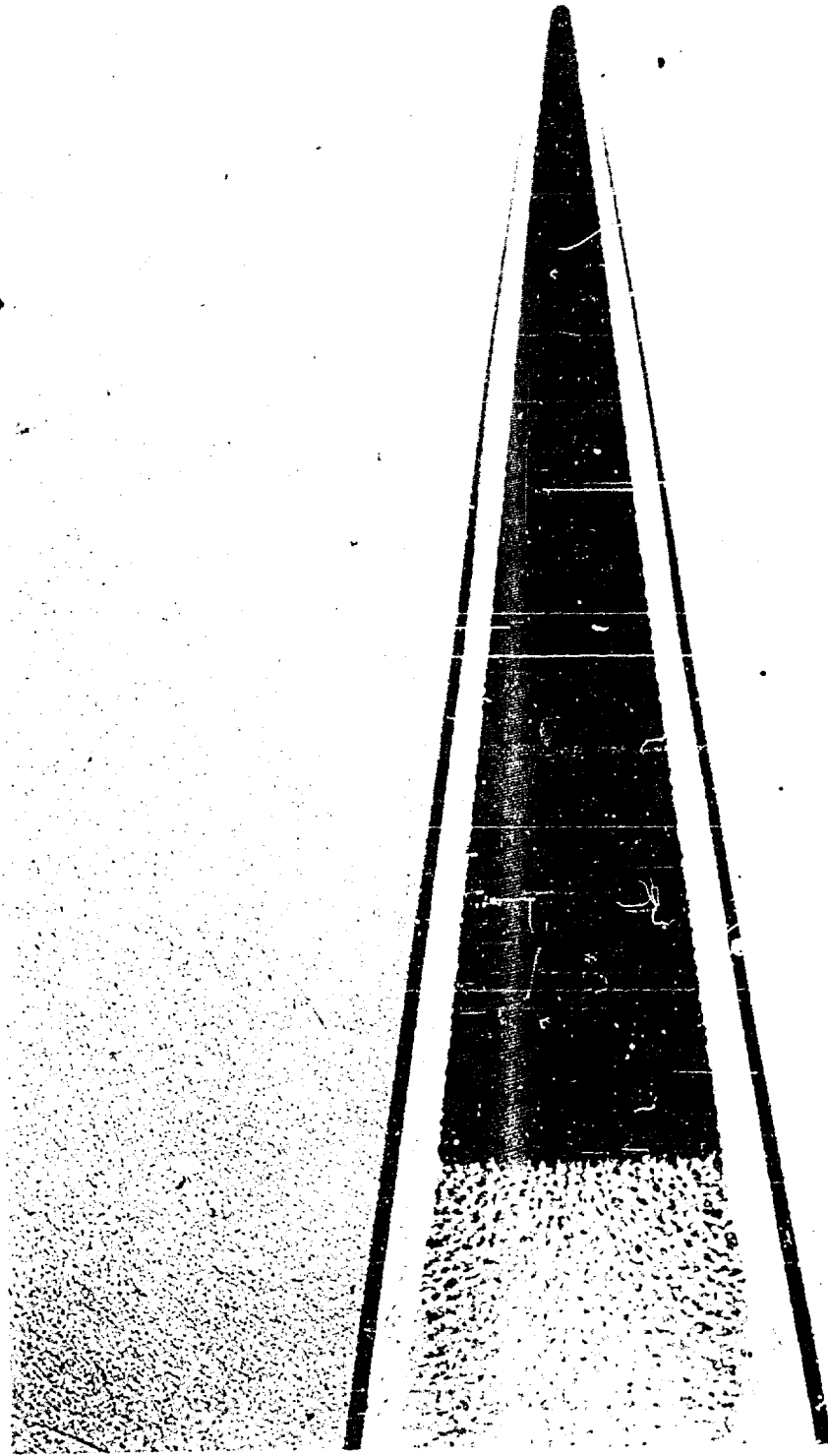


FIG. 2.8 SHADOWGRAPH OF MODEL FLYING AT  
STATION 360, MACH NUMBER 9.53  
SHOT No. 710.

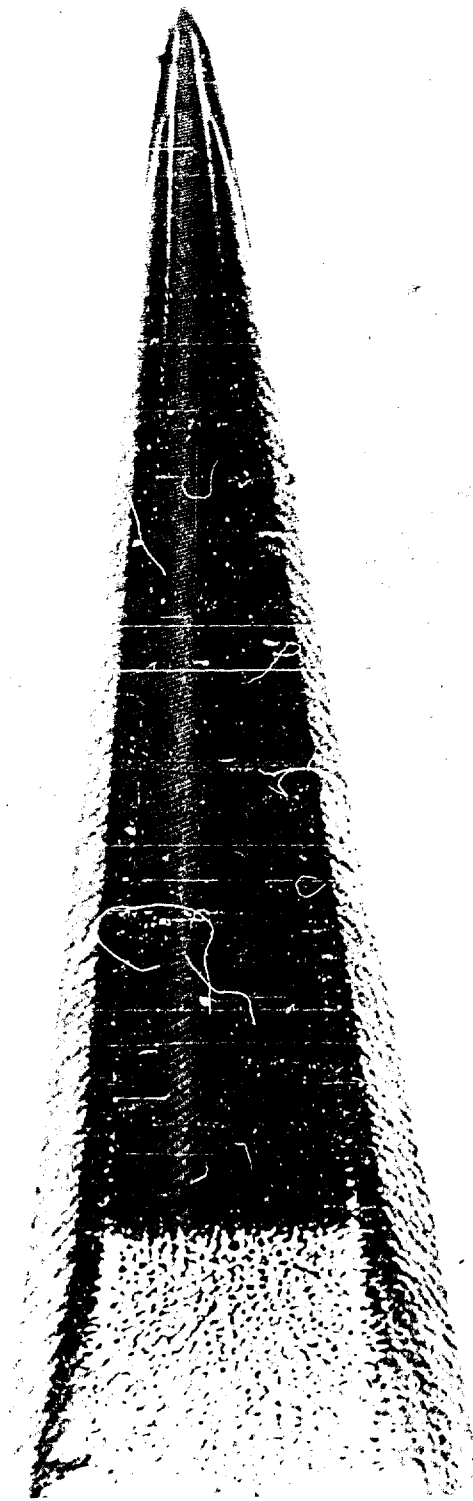


FIG. 2.9 SCHLIEREN OF MODEL FLYING AT  
STATION 245. MACH NUMBER 9.53  
SHOT -No. 710.

#### IV. STATUS OF NOL BALLISTICS RANGE PROGRAMS (cont.)

##### B. Task 3.0 Effect of High Heat Transfer Rates on Boundary-Layer Transition

The current ABRES boundary-layer transition program has been planned to investigate the effect of temperature ratio on boundary-layer stability at Mach number 8. The test configuration is a sharp 10-degree total-angle cone and is shown in figure 3.1. Similar tests have been conducted at NOL on the same configuration at Mach numbers 3 and 5, and the results have been reported in references (3.1) and (3.2). In these tests, the ratio of wall temperature of the model to the recovery temperature of the air is varied by varying the velocity of the model. As the model velocity is increased, the speed of sound is increased an appropriate amount by increasing the ambient temperature in the range to keep the Mach number constant. An electrical heater is installed within the range to control the air temperature in a 20-foot section of the range.

As mentioned in the previous quarterly progress report, the first launchings failed due to excessive luminosity. The surface temperature of the thin titanium fins was increased by aerodynamic heating sufficiently to cause the fins to burn. It was possible to locate the source of the luminosity by monitoring the light intensity with a photoelectric pickup as the model passed a data station. A typical oscilloscope record of the variation in the light intensity is presented in figure 3.2. A movement along the curve from the left to the right represents an increase in time while a downward displacement of the curve represents an increase in light intensity. This results in an increase in voltage generated at the photoelectric pickup. The intensity level of the light screen used to trigger the photographic station upon arrival of the model is shown by the initially horizontal portion of the curve. After approximately 900 microseconds, there is a slight increase in intensity as the tip of the model begins to move in front of the pickup. As the glowing tip moves past the pickup the intensity decreases indicating the presence of the cooler body which is not luminous. After a sufficient time interval to allow the fins to move in front of the pickup, however, the intensity increases drastically indicating that the fins are burning.

At the lower velocities it was possible to reduce the luminosity sufficiently by evacuating the range to approximately 10 mm Hg and then filling the range with nitrogen to obtain the desired operating pressure. However, at velocities in excess of 10,000 feet per second luminosity again became a problem.

At this velocity the range temperature had to be increased to approximately 200°F to obtain a free-stream Mach number of 8. It was possible to extend the data range of these models by two modifications. First, the fins were trimmed in size so that the bow shock did not intersect the fin surface. This removed the fin from the zone of high heating immediately behind the shock. The second modification was to plate the fin surface with copper. This served a double purpose. Since copper is a better conductor than titanium, it transferred heat away from the stagnation region faster and helped to reduce the temperature in the tip and edge regions. Also, since enough copper was added to nearly double the thickness of the fin, the heat sink capacity of the fin was greatly increased. With these modifications, it was possible to obtain velocities as high as 11,500 feet per second with range temperatures of approximately 400°F. It does not appear feasible to launch these models at higher velocities in view of the heating problems associated with the fins. In order to obtain the proposed minimum temperature ratio of 0.036 at a Mach number of 8, the launch velocity required is approximately 14,000 feet per second with a range temperature of 800°F. Data testing for maximum conditions of heating has, therefore, been rescheduled for August 1965 when the heat transfer section (heater) will be again installed in the range.

Development effort will continue in order to develop new model configurations that will meet maximum requirements. Although several methods are being considered, it now appears that some fin area will be necessary in order to keep model yaw angles within acceptable limits. This requirement will be discussed later in this report.

At present the data obtained from the lower velocity Mach number 8 launchings are being reduced. In addition to the standard range data reduction techniques which determine the model velocity, Mach number, and angle of attack, an additional analysis is being made to determine the transition Reynolds number and to compare these results with similar tests made at other Mach numbers.

The data are reduced to a local transition Reynolds number based on the local flow conditions and the length of laminar flow on the body. In order to obtain the local flow properties, it is first necessary to determine the free-stream conditions. The range pressure is measured directly by pressure gages. The free-stream velocity is determined at each data station by measuring the time required for the model to travel from one data station to the next. Two thermocouples are located at each data station within the heated section of the range to measure the ambient temperature at the stations. The free-stream density can be calculated from the equation of

state since both the pressure and temperature are known. Using these free-stream conditions, the corresponding local properties can be calculated with the aid of tables of flow properties for yawed cones (reference (3.3)) and tables of isentropic flow (reference (3.4)). Two rays of the boundary layer can be seen on each shadowgraph photograph, one on the windward surface of the model and one on the leeward surface. In general, the model is at some angle of attack to the free stream. In order to obtain the local flow properties along each ray, the angular orientation of the ray with respect to the pitching plane is determined from the horizontal and vertical components of the angle of attack. After the orientation of the ray has been determined, the local flow conditions are determined from references (3.3) and (3.4).

The location of boundary-layer transition is determined optically from the spark shadowgraph photographs taken of the model during its flight down the range. The photographic plates used in these tests consist of film emulsion on 14 by 17 inch glass plates. Photographs are obtained of the model at each data station. The location of transition is measured from the tip of the image directly from the glass photographic plate. Examples of the shadowgraph photographs obtained in this program are shown in figures 3.3a and 3.3b. It should be noted that in figure 3.3a the model is at a very low angle of attack and at this condition the location of transition is approximately the same distance back from the tip on both the top and bottom rays. However, in figure 3.3b where the model is at a larger angle of attack, it can be seen that the length of laminar flow on the windward ray is more than double the length of laminar flow on the leeward ray. This illustrates the need for maintaining very low angles of attack.

During the next quarter the analysis of the data from successful launchings will be completed. New model configurations will be designed to keep luminosity and yaw angle within acceptable limits. Preliminary development shots will be made prior to installation of the heater, and it is expected that the remaining data firings can be successfully completed during the final quarter of the program.



### References

- 3.1 Lyons, Jr., W. C., and Sheetz, Jr., N. W., "Free-Flight Experimental Investigations of the Effect of Boundary Layer Cooling on Transition," NOLTR 61-83, U. S. Naval Ordnance Laboratory (1961).
- 3.2 Sheetz, Jr., N. W., "Free-Flight Boundary-Layer Transition Investigations at Hypersonic Speeds," AIAA Paper No. 65-127, presented Second Aerospace Sciences Meeting, January 1965.
- 3.3 Staff of the Computing Section, Center of Analysis (under direction of Zdenek Kopal), "Tables of Supersonic Flow Around Yawing Cones," M.I.T. Technical Report No. 3 (1947).
- 3.4 Ames Research Staff, "Equations, Tables, and Charts for Compressible Flow," NACA Report 1135 (1953).

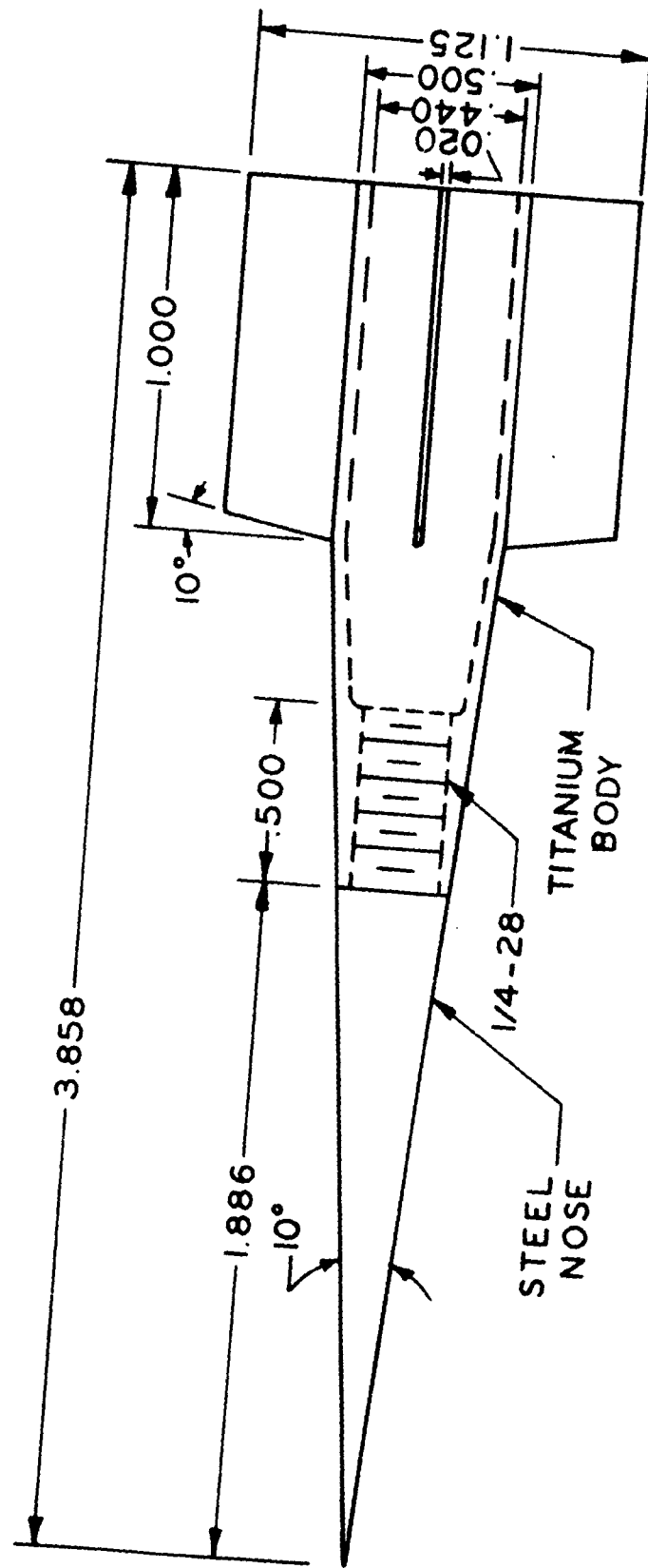


FIG. 3.1 10° FINNED CONE RANGE MODEL

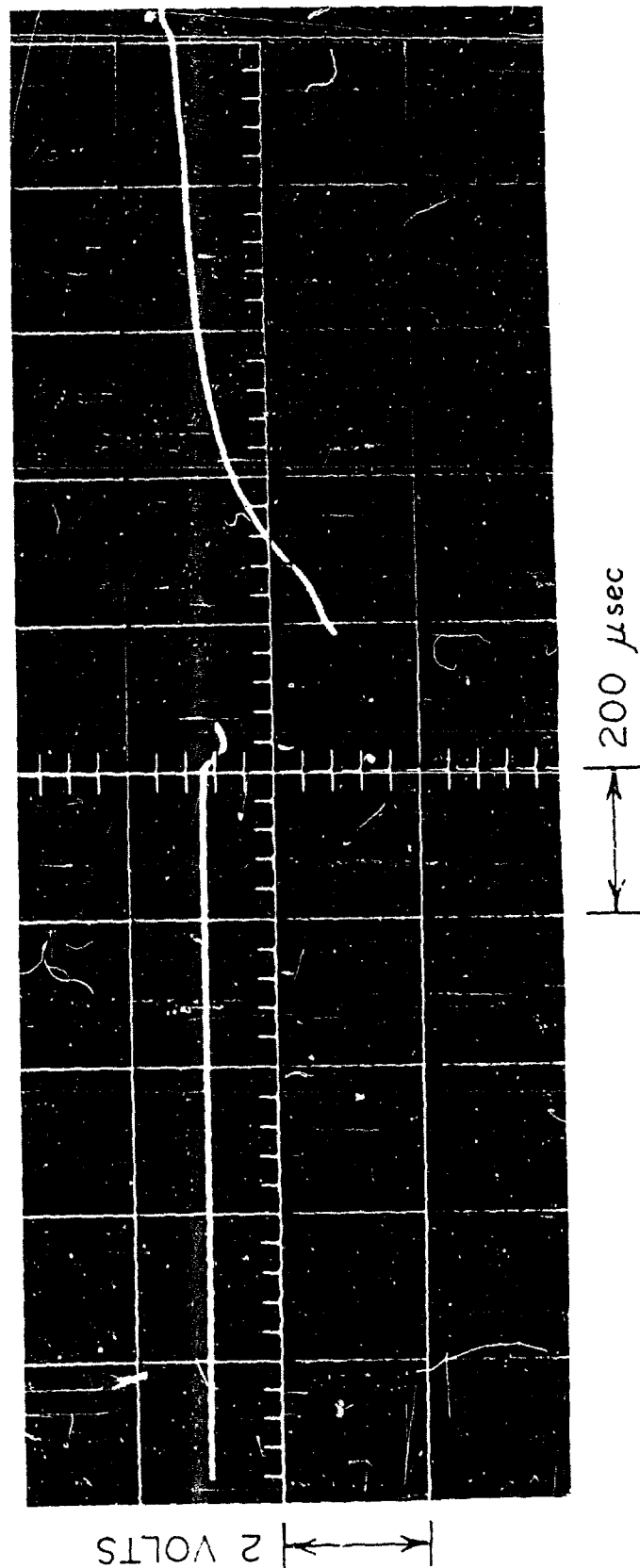


FIG. 3.2 VARIATION IN LIGHT INTENSITY AS MODEL PASSES  
DATA STATION

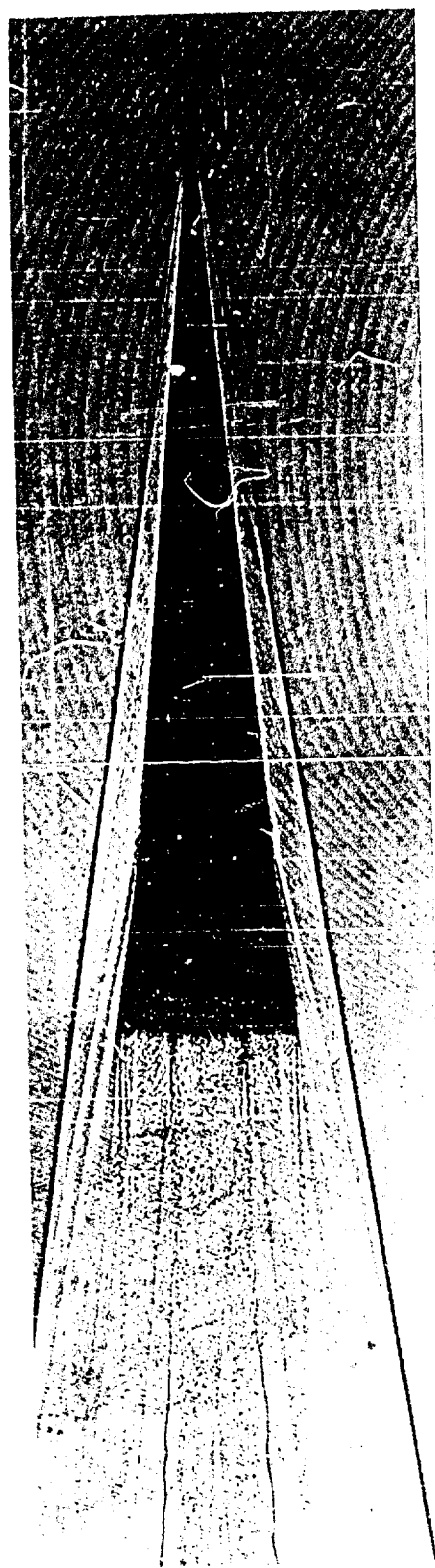


FIG. 3.3a SHADOWGRAPH OF MODEL AT LOW ANGLE OF ATTACK  
WITH TRANSITION OCCURRING SYMMETRICALLY

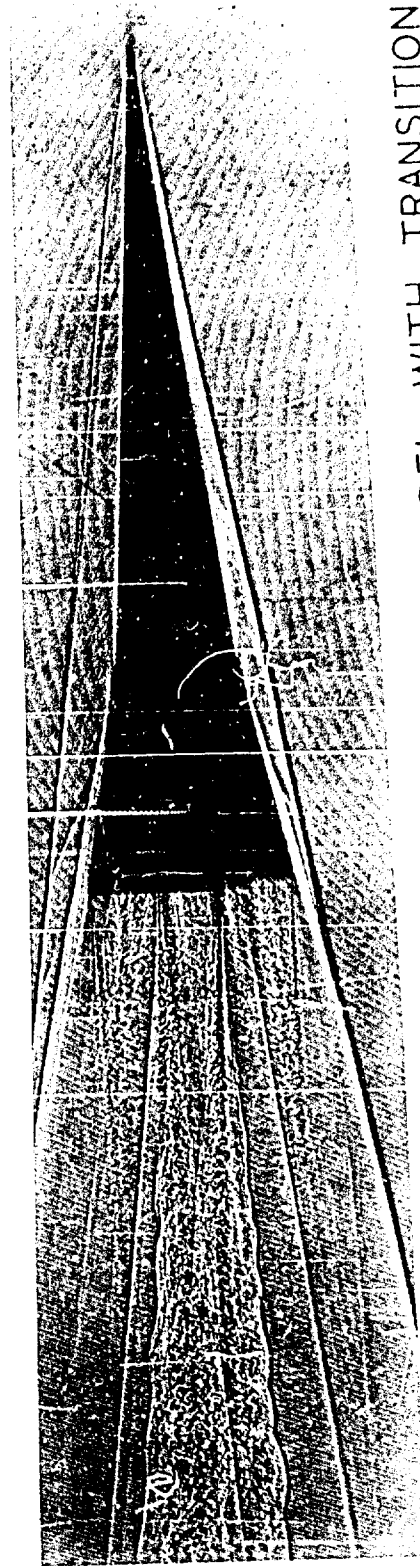


FIG. 3.3b SHADOWGRAPH OF YAWING MODEL WITH TRANSITION  
OCCURRING UNSYMMETRICALLY

#### IV. STATUS OF NOL BALLISTICS RANGE PROGRAMS (cont.)

##### C. Task 4.0 Body-Scale Effects on the Aerodynamic Characteristics of Wakes

In ballistic missile and space flight technology it is very important to know whether the wake flow behind the entering vehicle is laminar or turbulent. A great deal of experimental information on laminar to turbulent flow transition has been obtained for small bodies in laboratory tests. To ascertain the validity of extending small-scale laboratory test results to full-scale flight vehicle predictions, it was decided to conduct a ballistics range firing program in which the model sizes varied by a factor of 14. The model configuration being investigated is a 9-degree half-angle cone with 0.05 nose to base radius ratio. The tests are to be conducted at Mach number 10.

There are two parts to this program. In one, the wake transition characteristics are to be investigated over the largest possible Reynolds number range. The smallest body, which is a 0.1-inch base diameter cone, will be tested at the lowest possible range pressure, and the largest body, which is a 1.4-inch base diameter cone, will be tested at the highest, possible range pressure. This should result in a free-stream Reynolds number variation between approximately  $10^4$  and  $10^6$  based on body diameter. In the second part of the program the wake transition characteristics will be determined at a fixed body Reynolds number by adjusting the range pressure for various base diameter cones.

To date, four 1.4-inch diameter cones have been fired in the Hyperballistics Range No. 4. Figure 4.1 is a shadowgraph of one of these cones in flight. Useful wake transition information can be obtained from three of the shots. These data established the highest body Reynolds number for this investigation ( $R_e = 1 \times 10^6$ ). In the Pressurized Ballistics Range No. 3, to date only model development firings have been made. A shadowgraph from one of these shots is shown in figure 4.2. Two 0.6-inch, two 0.3-inch, and two 0.1-inch base diameter cones were fired. Fair data can be obtained from one of each of the 0.3 and 0.6-inch base diameter shots. An analysis of these data indicates that for a fixed body Reynolds number the free-stream wake transition Reynolds number is constant when the body size differs by a factor of 2.3. This analysis also indicates that the wake transition Reynolds number increases slightly with an increase in the body Reynolds number. The body Reynolds number range here is between  $5 \times 10^5$  and  $10^6$ . These statements concerning transition characteristics have been

based upon limited data and should be considered preliminary. Additional firings are scheduled in the Pressurized Ballistics Range No. 3 during May. The models and sabots for these firings have been manufactured.

It is planned to have a sensitive schlieren system operational in the Pressurized Ballistics Range No. 3 when the May firings are made. From the schlieren photographs it is hoped to obtain important information about the base flow geometry.



FIG. 4.1 SHADOWGRAPH OF CONE FOR BODY SCALE EFFECTS  
INVESTIGATION.  $M_{\infty} = 11.1$   $R_{\infty d} = 9.28 \times 10^5$



FIG. 4.2 SHADOWGRAPH OF CONE FOR BODY SCALE EFFECTS  
INVESTIGATION.  $M_{\infty} = 9.6$   $R_{\infty d} = 5.83 \times 10^5$



#### IV. STATUS OF NOL BALLISTICS RANGE PROGRAMS (cont.)

##### D. Task 5.0 The Effect of Heat Transfer on the Aerodynamic Characteristics of Wakes

Among the various experimental facilities suitable for hypersonic investigations, only the ballistics ranges are capable of simulating the wall to stagnation enthalpy ratios that exist in flows around hypervelocity re-entry vehicles. This capability used with a special section in the Pressurized Ballistics Range No. 3 where the ambient gas temperature can be closely controlled makes it possible to investigate the effects of varying stagnation enthalpy on hypersonic base and wake flow characteristics. In this special heated section of the range the ambient temperature can be varied between approximately 80 and 850°F. This equipment is also used for the experiments conducted under Task 3.0. In order to investigate the stagnation enthalpy effects on the flow characteristics at a given fixed Mach number, the models are launched at different velocities producing different appropriate amounts of kinetic energy in the flow. Meanwhile, the temperature in the heated section of the range is adjusted so that the flight Mach number remains at the desired value.

The present program was planned to investigate the wall to stagnation enthalpy ratio effects on the base flow geometry and wake flow laminar to turbulent transition characteristics. The Mach number chosen was approximately 8.5 with wall to stagnation enthalpy ratios between 0.03 and 0.075. The model configuration for this study is a 9-degree half-angle cone with a 0.05 nose to base radius ratio.

The range firings for this program have been completed. A total of 21 shots were fired. In figure 5.1 is shown a shadowgraph of a cone flying in the heated section of the range. The ambient temperature is 400°F, the Mach number  $M_\infty = 6.7$ , and the body Reynolds number  $R_{bd} = 2.4 \times 10^5$ . Figure 5.2 shows the same cone flying in the unheated section of the range where the ambient temperature is 75°F. The Mach number here is 8.42 and the body Reynolds number  $5.45 \times 10^5$ . The shadowgraph plates obtained from this program have been measured. The measurements include the distance from the base of the cone to the recompression shock waves, and the distances from the base of the cone to the first appearance of laminar waves and fully turbulent flow in the viscous wake. Most of the data have been reduced, and the results are being analyzed.

The effect of varying the stagnation enthalpy on the wake transition Reynolds numbers is shown in figure 5.3. The wake transition Reynolds numbers  $R_{x_1}$  and  $R_{x_2}$  are defined as

the free-stream unit Reynolds numbers multiplied by  $x_1$ , the distance from the base of the cone to the appearance of laminar waves and  $x_2$ , the distance from the base of the cone to the onset of fully turbulent flow in the viscous wake. In computing the ratio of the wall to stagnation enthalpy, the wall enthalpy  $h_w$  has been assumed to be constant and equal to the ambient room enthalpy. For the very short flight times this is a good assumption except for the tip of the cone region. Therefore, in this case a variation in the ratio  $h_w/h_o$  really involves only a stagnation enthalpy variation.

At this time only preliminary conclusions can be drawn about the results in figure 5.3. Not all the results are yet available and there was very little time to study and analyze the results that are presented. From figure 5.3 it appears that for both wake transition Reynolds numbers there is no effect of the wall to stagnation enthalpy ratio in the region between  $h_w/h_o = 0.04$  to  $0.075$ . However, at  $h_w/h_o$  there appears an appreciable decrease in the  $R_{\infty x_1}$  and some decrease in  $R_{\infty x_2}$ . Whether such a result is to be expected is not clear at the present time.

The data obtained on base flow geometry and some additional wake transition readings are being reduced and analyzed.



FIG. 5.1 SHADOWGRAPH OF A CONE INSIDE THE HEATED SECTION  
OF THE RANGE.  $M_{\infty} = 6.7$   $R_{\infty d} = 2.45 \times 10^5$   $R_{\infty x_2} = 1.03 \times 10^6$

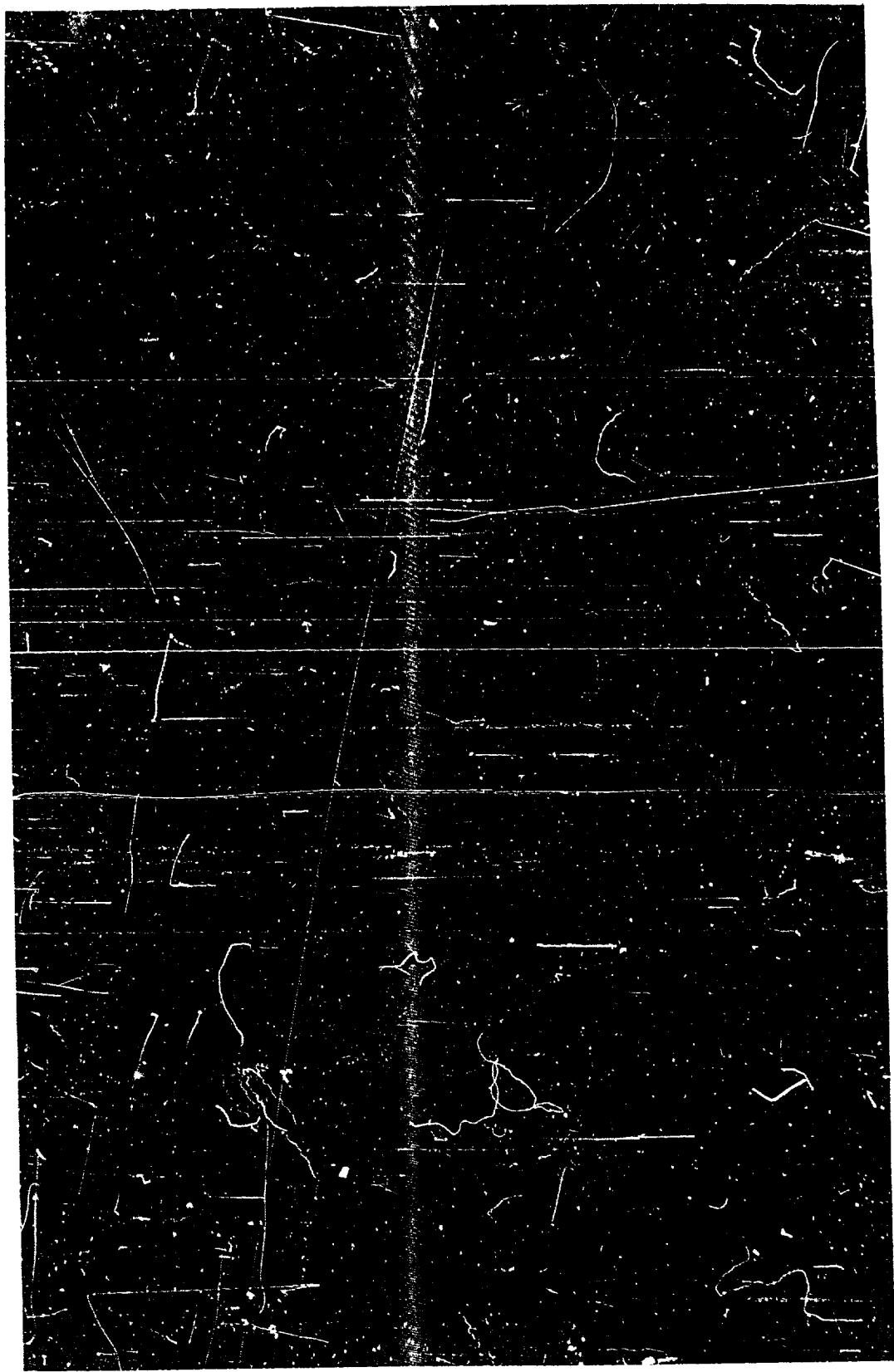


FIG. 5.2 SHADOWGRAPH OF THE SAME CONE IN THE REGULAR SECTION OF THE RANGE.  $M_{\infty} = 8.42$   $R_{\infty d} = 5.5 \times 10^5$   $R_{\infty x_2} = 2.64 \times 10^6$

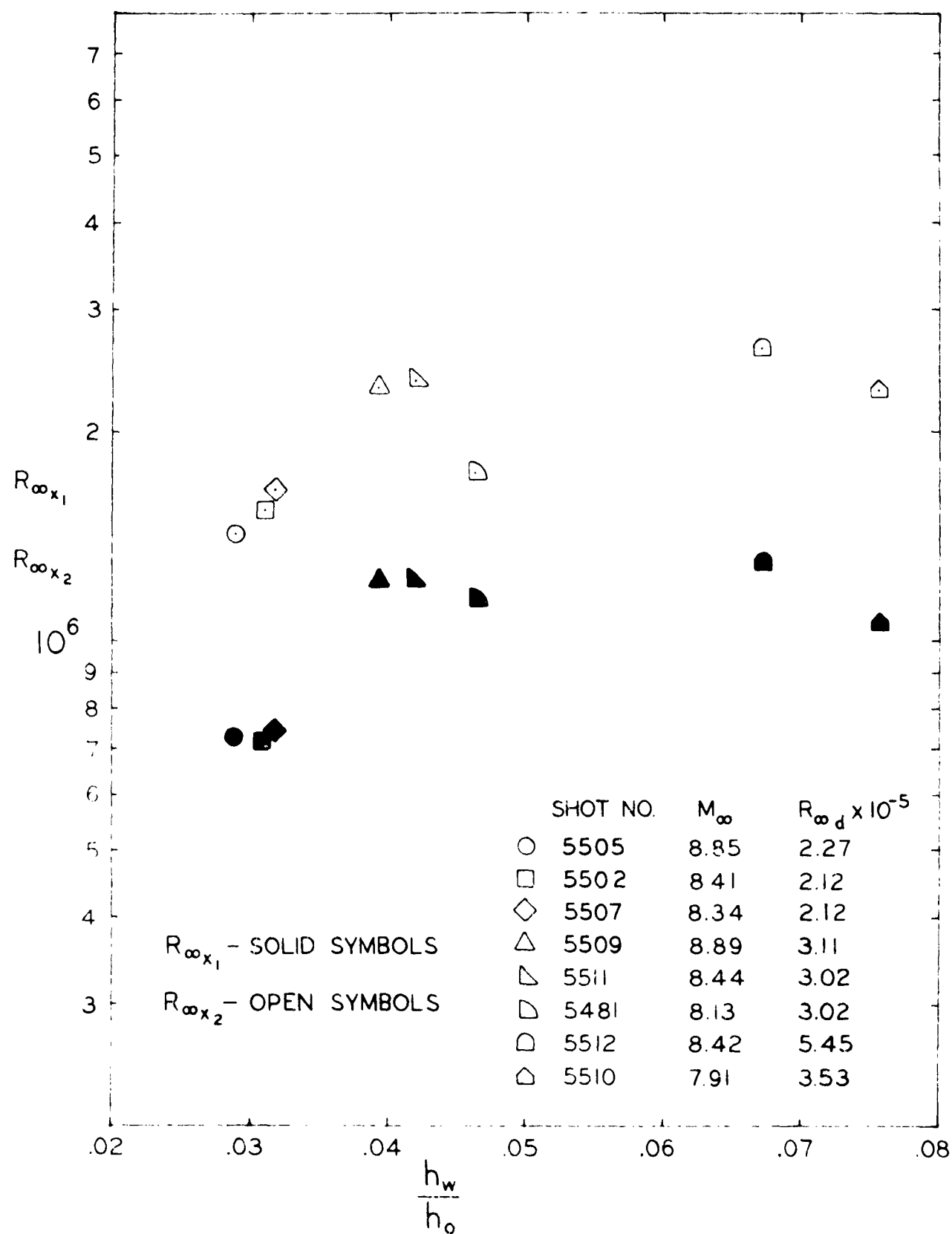


FIG. 5.3 EFFECT OF STAGNATION ENTHALPY ON WAKE TRANSITION REYNOLDS NUMBERS